EQA - International Journal of Environmental Quality
ISSN 2281-4485 - Vol. 63 (2024): 26-40
Journal homepage: https://eqa.unibo.it/

published by

Optimizing courtyard orientation for wind-driven ventilation in hot-arid climates: a case study from Egypt

Rabab S. Qataya[1*], Mady Ahmed Mohamed[1,2], Hussien AlShanwany[1], Shimaa Sabour[1,3]

[1] Department of Architecture, Faculty of Engineering, Zagazig University, Zagazig, Egypt
[2] Department of Architecture, Effat University, Jeddah, Kingdom of Saudi Arabia
[3] Department of Architecture, High Institute of Engineering and Technology, Al-Obour, Egypt

* Corresponding author Email: rskataya@eng.zu.edu.eg

Article info
Received 17/7/2024; received in revised form 24/7/2024; accepted 1/8/2024
DOI: 10.6092/issn.2281-4485/20043

Abstract
Nowadays, there is an increasing demand for buildings that offer ideal ventilation and thermal conditions, particularly in hot-arid regions. Courtyards emerge as pivotal elements facilitating enhanced airflow and utilizing natural energy, resulting in reducing energy consumption in addition to controlling the pressure created by the wind. In response to the motivation of optimizing building performance in the face of harsh environmental challenges, our study aims to investigate how different courtyard orientations affect airflow patterns and ventilation performance in an educational building model located in Cairo and Delta region. The building, designed for the Pre-university education phase by the General Authority for Educational Buildings (GAEB), as a free-running building. Using a Computational Fluid Dynamics (CFD) simulations through ANSYS-Fluent software, we performed a parametric analysis testing four different orientations (0°, 15°, 30°, and 45°) in the northwest direction to identify the optimal orientation for enhancing ventilation performance. The results consistently indicated that the 0° scenario yielded the best results, followed notably by the 15° scenario which outperformed others by demonstrating superior airflow patterns and pressure differences conducive to enhanced ventilation rates. The 45° scenario was identified as the least favorable result among the four scenarios. These findings provide valuable methodological insights for architects and policymakers seeking to optimize natural ventilation strategies within Egypt's climates.

Keywords
Courtyard Orientation; Airflow Patterns; CFD Simulation; Hot-Arid Climate; Differential Pressure.

Introduction

Egypt's distinctive geographical location, between latitudes 23° to 32° , exposes it to a "Hot-Arid desert" climate type (BWh) in the south and central regions and a "Semi-Arid Hot" climate type (BSh) along the coasts, according to the Köppen Climate Classification (Saleem et al., 2016). While Köppen's classification is useful for macroclimate analysis, it is less effective for building design due to its general nature. Accurate microclimate assessment is essential for selecting optimal climate-oriented strategies during the initial phases of the design process (Mahmoud, 2011). Over the microclimate scale, Egypt features diverse climatic zones, from the hot deserts of the Western Sahara and southern regions to the colder St. Catherine Mountains in Sinai (Mahmoud, 2011). Housing and Building National Research Center (HBRC) and the Egyptian Residential Energy Code (EREC) have categorized Egypt into eight distinct climatic zones, as illustrated in Figure 1 (Mi-

DOI: 10.6092/issn.2281-4485/20043

nistry of Housing, 2005). Each zone exhibits specific attributes, contributing to varied environmental, cultural, and climate conditions that significantly impact the design process. Therefore, it is erroneous to assume that a building in Alexandria would exhibit the same performance as one in Cairo or Asyut (Abdin and Mahmoud, 2017). Consequently, it becomes imperative to study the specific climate characteristics of each region, define the adopted design strategies, and examine the role of each strategy and assessing their impact on achieving comfort for occupants (Mahmoud, 2011). Mohamed (2010) has undertaken a classification of the main strategies applicable in Egypt, categorizing them primarily into three funda-mental strategies: passive solar design, evaporative cooling, and natural ventilation. One of the most crucial design elements utilized when dealing with the challenges posed by this climate is the courtyard (Givoni, 1998 , Mohamed, 2010). Courtyards have long been used in Egyptian building design to protect against extreme weather by providing shading and enhancing natural ventilation (Almajidi and Hameed, 2020 , Soflaei et al., 2020). These courtyards vary in orientation, dimensions, and proportions based on site-specific attributes and external influences (Ibrahim et al., 2021). These attributes are harness-sed to fulfill various purposes that might be environ-mental, cultural, social, and functional (Almajidi and Hameed, 2020; Ibrahim et al., 2021). Courtyard buildings' forms

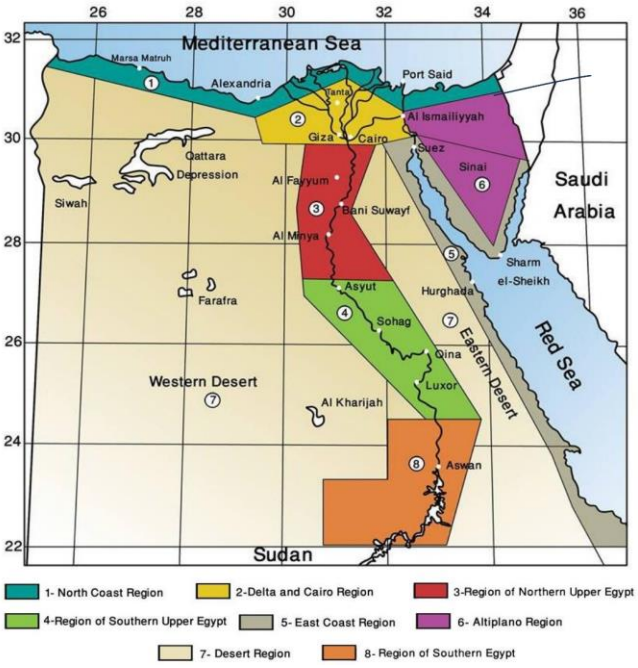

Figure 1. *Classification of climatic zones in Egypt (Saleem et al., 2016)*

can vary based on design requirements, with a general preference for either multi-court or single-court configurations over linear types. Moreover, courtyard design necessitates the integration of various elements, including shading devices, water features, and vegetation. These compo-nents aid in cooling through evaporation, reducing temperatures, and enhancing airflow dynamics. Furthermore, other architectural elements such as Takhtaboush, roof design, and building materials are equally pivotal and their absence compromises the efficacy of courtyard design (Mohamed, 2010; Taleb and Abumoeilak, 2021 , Prakash, 2023). While pre-vious research in Egypt has primarily focused on courtyard shading and passive solar design, less attention has been given to optimi-zing courtyard aerodynamics for natural ventilation (Bienvenido-Huertas et al., 2023). Therefore, this stu-dy will focus on analyzing wind environments in courtyard buildings and the impact of orientation on airflow patterns and ventilation performance. Courtyards facilitate air exchange with urban areas and building interiors, influenced by wind-induced forces due to pressure differences on building sides. Higher pressure on the windward side and lower pressure on the leeward side create airflow. Temperature differ-rences within the building also cause air circulation through buoyancy forces, known as thermal buoyancy or the stack effect (Abdelhady, 2021). The design considerations for courtyard buildings exhibit variability in terms of previously mentioned parameters according to the climatic characteristics of each region (Taleb et al., 2020). Numerical simulations are commonly used to assess wind environments around buildings. While CFD is cost-effective and time-efficient, caution is needed when empirical data is lacking (Mohamed and El-Amin, 2022). Within the main scope of the research to study airflow patterns within courtyard buildings, particularly in Egypt's climate. An educational building model utilizing natural ventilation through a courtyard was selected. The General Authority for Educational Buildings (GAEB) in Egypt uses standard design models across the country, not accounting for regional climatic variations, leading to unhealthy and uncomfortable school environments (Hamed, 2023). GAEB's code does not provide specific guidelines for optimizing natural ventilation through building orientation (GAEB, 2023). Therefore, this research will primarily aim to propose optimal orientation for courtyard buildings under Egyptian

DOI: 10.6092/issn.2281-4485/20043

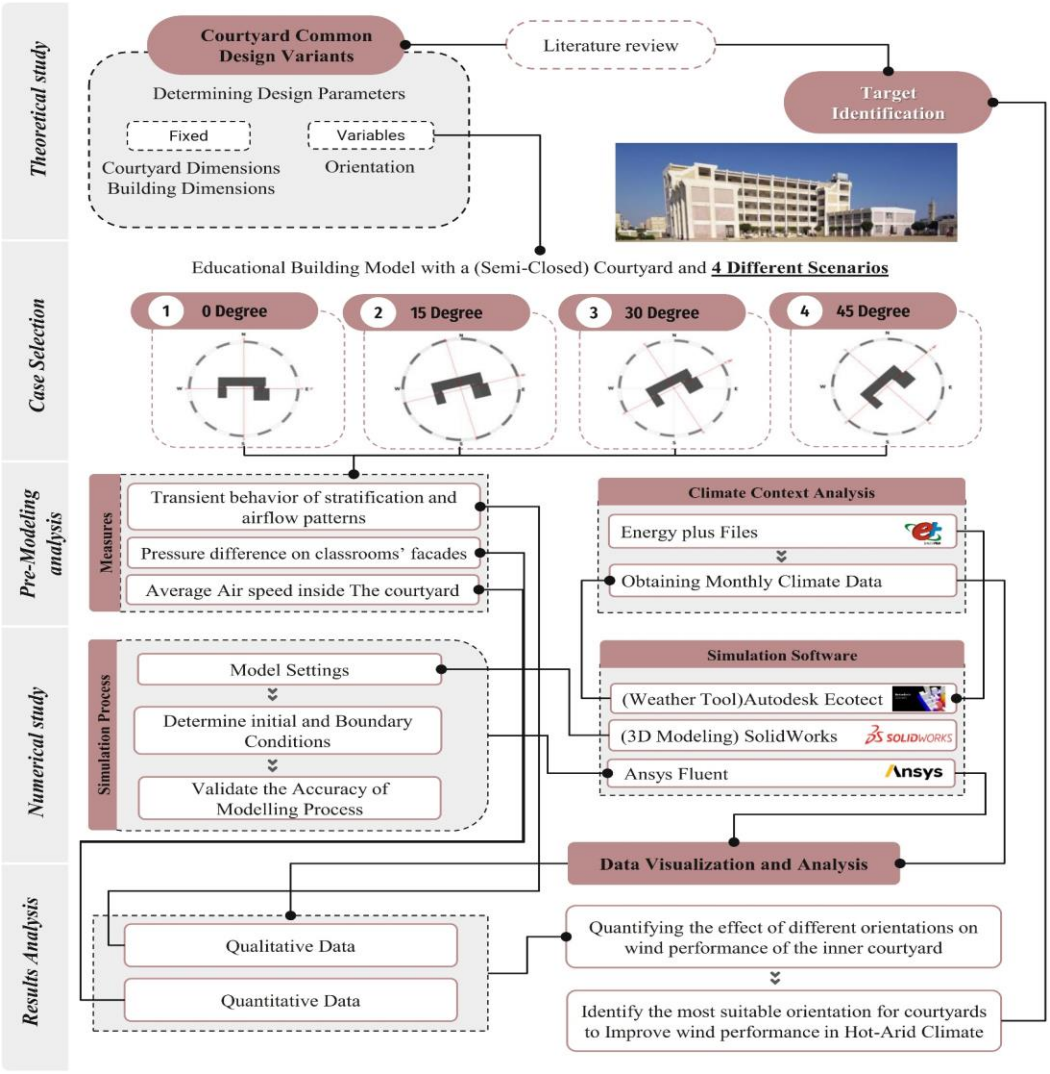

Figure 2
Detailed research methodology

climatic conditions using CFD simulations, a reliable method for predicting natural ventilation performance and wind characteristics. The study details the steps for conducting trustworthy CFD simulations.

Materials and Methods

This research incorporates a CFD simu-lation, as illustrated in Figure 2, to investigate how different courtyard orientations affect air velocity and movement within a semi-enclosed courtyard of an educational building model. Also, it aims to predict classroom ventilation efficiency by calculating the average wind pressure differences between the classrooms' main facades (Yawen et al., 2023). Based on Bernoulli's principle, pressure differences create airflow, with high pressure on the windward side and low pressure behind it (Mohamed and El-Amin, 2022). Additionally, to meet ASHRAE standards, wind speed inside the courtyard must exceed 5 m/s (American Society of Heating and Air-Conditioning, 2017). The model is located in Cairo and Delta.clima tic region. This area was chosen because it has the highest number of schools in Egypt (CAPMAS). The numerical investigation of four orientation scenarios (0°, 15°, 30°, and 45° in the northwest direction) was conducted using ANSYS-Fluent 2022. These orienta-tions were selected based on previous literature recommending optimal orientations for natural ventilation of courtyard buildings in hot-arid regions, falling within the range of 0° to 45° in the northwest direction (Wazeri, 2002 , Soflaei et al., 2020). The study considers varying wind speeds and directions throughout the 12 months of 2023, focu-sing on wind-induced ventilation and excluding buoyancy effects, and heat gains/losses. Simulations were conducted on a desktop with a 9-core Intel® Core™ i9-9900K @ 3.6 GHz processor, 64 GB installed memory, and a 64-bit operating system.

DOI: 10.6092/issn.2281-4485/20043

Climatic context analysis

The weather data for the selected climate region was downloaded from the EnergyPlus website in EPW format and analysed using Ecotect software's Weather Tool. The comprehensive analysis of a year's weather data for the Cairo and Delta region, classified as hot-arid by Köppen, was conducted using data from a weather station located 10 meters above ground at Cairo International Airport, operated by the Egypt Observatory (Afandi, 2014). The dataset includes detailed records of wind speed and direction, offering valuable insights into the region's climate. Based on observations from the statistical data of wind included in Figure 3, several noteworthy patterns were revealed. Wind direction shows distinct seasonality: in summer, winds primarily come from the north, while in winter, south and south-westerly winds prevail. Notably, similar wind directions (350°) were observed during summer months. The wind speed displayed temporal variations, reaching the highest mean values occurring during the spring season, see Table 1. This highlights the necessity of including data for all months instead of relying on specific days to study wind flow patterns and speeds, as that can result in inaccurate findings. Using the Weather Tool and Olgay Charts, the study highlights that natural ventilation significantly enhances building thermal performance, especially during summer, see Figure 2. This analysis facilitates informed decisions on passive techniques and strategies.

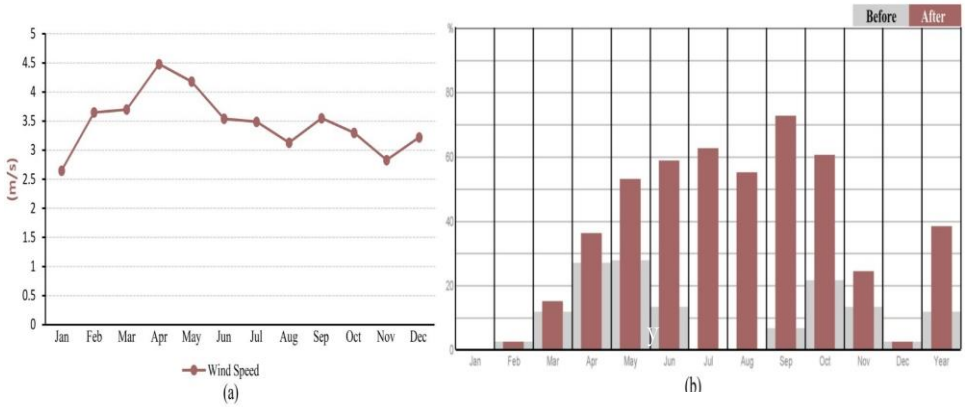

Figure 3
(a) Monthly average data of wind speed for the Cairo and Delta climatic region in 2023 (b) Effect of applying natural ventilation strategy for enhancing thermal comfort in Cairo-Delta region, after Weather Tool – Autodesk Ecotect software

Assumptions and description of the model

The case study building is one of several educational models implemented by GAEB in Egypt, exclusively for the Pre-university education phase. It consists of five floors (ground + 4) with 33 classrooms, relying primarily on natural ventilation. All classrooms use a cross-ventilation strategy and are single-loaded, as shown in Figure 4. The dimensions of the building (Length – L, Width – W) are 56 m, and 28.5 m respectively, with a total height of 18.35 m. Additionally, it includes a semi-enclosed rectangular (U-shape) courtyard space of width 19.35 m, length 32.5 m, and height 18.35 m with an aspect ratio of 0.95 and a roof inclined at 3° towards the courtyard (GAEB, 2023). The numerical analysis was conducted under "closed window" conditions to simulate wind flow patterns around the building. The building's geometry was modeled using SolidWorks software and then loaded into Ansys Design Modeler to incorporate the surrounding atmosphere as an additional envelope. The building model was generated using the Boolean

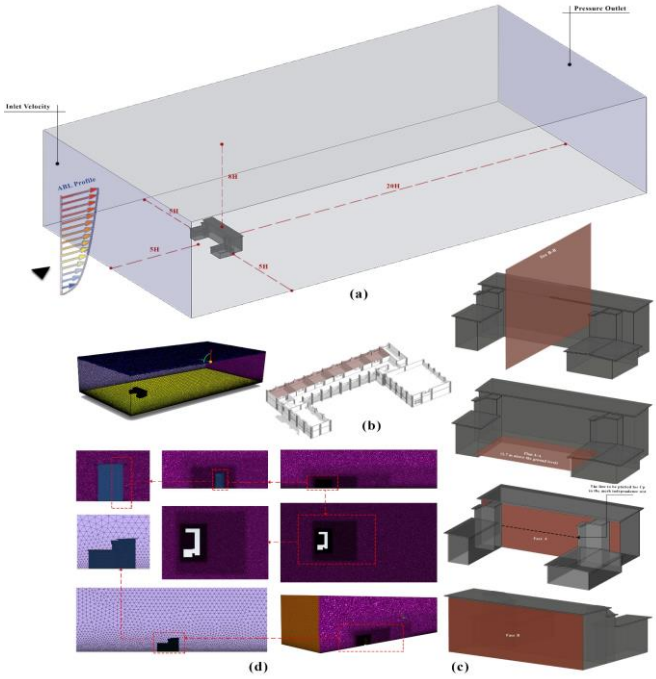

Figure 4. a) Dimensions of the computational domain – (b) The location of the classrooms within the building mass – (c) Position of sec B-B, plan A-A, Face A, and Face B within the building, respectively from top to bottom – (d) Mesh refinement process

DOI: 10.6092/issn.2281-4485/20043

algorithm (i.e., subtracting the solid domain from the external fluid domain (Obeidat et al., 2023)), simplifying it to an isolated rectangular building without any openings, external details, sunshades, portico, and surrounding trees. Subsequently, grids were generated on surfaces using the "mesh tool" in Ansys. Average air velocity and airflow patterns inside the courtyard at the level of 1.7 m "plan A-A" (based on the height of a normal person standing (Tang et al., 2023)) will be investigated along with section B-B in the middle of the courtyard building, highlighted with the red-shaded area, as shown in Figure 4. Additionally, pressure differences on classroom surfaces (Faces A and B) will be calculated.

CFD Simulation and turbulence governing equations

In CFD for natural ventilation simulations, the choice of turbulence model is crucial for accuracy. Two prevalent approaches in CFD are commonly used: Reynolds-averaged Navier-Stokes (RANS) equations and Large Eddy Simulation (LES). RANS simulations are computationally efficient and versatile, often using 2-equation turbulence models like the standard k-epsilon (SKT), realizable k-epsilon (RLZ), renormalized group k-epsilon (RNG), and SST k-omega models (Zhang et al., 2020). Although RANS simulations are economical and less time-consuming (Blocken, 2018), their inability to resolve fluctuating flow variables leads to excluding turbulent components from the simulation (van Hooff et al., 2017). Additionally, they exhibit limitations in capturing phenomena such as vortex shedding and can lead to overpredictions of turbulent kinetic energy and flow recirculation near simulated buildings (Blocken, 2018). In contrast, LES provides a potential solution with its explicit modelling of larger eddies, offering more realistic flow data with higher computational requirements. Investigations utilizing RANS simulations have extensively studied the impact of building geometry, ventilation openings, and wind conditions on natural ventilation (van Hooff et al., 2017). Due to computer capabilities limitations and their robustness at a low cost, RANS equations were chosen for this research, supported by previous studies (van Hooff et al., 2017 , Stasi et al., 2024). The governing partial differential equations are solved using the Pressure-Based Navier-Stokes Equations (PBNS) solver, which forms the basis of the mathematical model. This model includes an eddy-viscosity formula solver for continuity and momentum, and a dissipation model equation, denoted as ε, for turbulence in the simulations. Eq. [1] and Eq. [2] represent the RANS equations, while Eq. [6] and Eq. [7] represent the turbulence equations (Serra, 2023).

Continuity equation:

$$\frac{\partial u_i}{\partial x_i} = 0 \qquad [1]$$

Momentum equation:

$$\frac{\partial u_i}{\partial t} + u_j \frac{\partial u_i}{\partial x_j} = \frac{1}{\rho} \frac{\partial}{\partial x_i} \left[-\rho + (\mu + \mu_t) \left(\frac{\partial u_i}{\partial x_j} + \frac{\partial u_j}{\partial x_i} \right) \right] \qquad [2]$$

Initial and boundary conditions

For CFD simulations, it is crucial to define boundary conditions on all surfaces of the computing domain, following best practice guidelines (Tominaga et al., 2008). A velocity-specified domain inlet is used to indicate airflow speed and direction, with monthly details in Table 1. At the outlet, the constant static pressure boundary condition is applied with a relative pressure set to 0 Pa, while the domain's operating pressure is maintained at 1 atm (i.e., 101,325 Pa). The simulation of the outdoor wind environment included the inflow boundary condition with a vertical velocity profile, reproducing an Atmospheric.

Table 1. *The recorded data of monthly average wind speed and direction through the year 2023, after Autodesk Ecotect software (months with duplicated wind directions have been highlighted with *)*

	January	February	March	April	May*	June	July*	August*	September	October*	November	December*
V (m/s)	2.65	3.65	3.7	4.48	4.18	3.54	3.49	3.13	3.55	3.3	2.83	3.22
Direction	190°	210°	30	40°	30°	350°	350°	350°	10°	40°	330°	210°

DOI: 10.6092/issn.2281-4485/20043

Boundary Layer (ABL) velocity profile along the building height. This profile was given by power laws equations in Eq. [3] (Tominaga et al., 2008 , Perén et al., 2015 , Prakash, 2023), with a ground roughness length of 0.5 (typical urban terrain in Cairo) (Elnabawi et al., 2017) and the atmospheric boundary layer friction velocity defined by Eq. [4] (Prakash, 2023). The reference wind speed was measured at the reference height of 10 m above the ground level with a von Kármán constant value of 0.42. This approach enhances the representativeness of the modeling results compared to real-life situations.

$$v\,(z) = \frac{v^*_{ABL}}{k} \cdot \ln\left(\frac{z + z_0}{z_0}\right) \quad [3]$$

$$v^*_{ABL} = k \cdot \frac{v_{ref}}{\ln\left(\frac{H_{ref} + z_0}{z_0}\right)} \quad [4]$$

These values were gathered within a user-defined function file for utilization as the parameters of gradient wind at the inlet boundary. The turbulent intensity characterizes the flow patterns resulting from wind separation, which is calculated using Eq. [5] (Perén et al., 2015).

$$I\,(z) = I_{10}\left(\frac{z}{10}\right)^{-\alpha} \quad [5]$$

The turbulent intensity *I10* measured at the reference height is specified as 0.39, while the surface roughness coefficient is set at 0.44 (GB50009, 2012). The profiles of turbulence kinetic energy, defined as the variance of fluctuations in velocity, and dissipation rate, representing the rate at which the velocity fluctuation dissipates with dimensions per unit time, are defined based on Eq. (6) and Eq. (7), respectively (Perén et al., 2015).

$$k\,(z) = \frac{{v^*_{ABL}}^2}{\sqrt{C_\mu}} \quad [6]$$

$$\varepsilon\,(z) = \frac{{v^*_{ABL}}^3}{k\,(z + z_0)} \quad [7]$$

The ε profile constants were set to $C = 0.09$ (Rivas et al., 2022). The CFD simulation assumptions involve a three-dimensional, fully turbulent, non-isothermal, and incompressible fluid flow to determine the average velocities inside the courtyard. Since the flow velocity is based on average monthly data, it is treated as a steady-state problem. Flow velocity, based on average monthly data, is treated as a steady-state problem. A standard wall function is incorporated to enhance study fidelity. Control equations are discretized using the finite volume method with a segregated implicit solver, employing a second-order upwind implicit scheme and a coupled scheme for pressure-velocity coupling. No-slip boundary conditions are applied as 'No Slip Walls'. The ground and building surfaces are defined as walls, while the top and sides of the fluid domain have 'symmetric' boundary conditions. For the lateral, upper, and downstream boundaries of the computational domain, the normal velocity component and normal gradients of tangential velocity components are set to zero. The building's walls are considered adiabatic boundaries (Mohamed and El-Amin, 2022 , Prakash, 2023). Under-relaxation strategies in FLUENT ensure convergence of variables like velocity, pressure, turbulent viscosity, kinetic energy, turbulent dissipation, and continuity. The default convergence criterion is set to [1-5] for the continuity equation and [1-6] for all other equations. The iteration process concludes once the convergence criterion is met, typically within 200 iterations, often satisfied before reaching this limit.

Domain and mesh generation

The models are positioned inside a computational domain following best-practice guidelines in CFD literature and recommendations (Tominaga et al., 2008). The domain dimensions were set relative to the courtyard building height (H): 5H upstream and laterally, 20H downstream, and 8H above, resulting in a size of L × W × H: 540 m × 260 m × 180 m, as illustrated in Figure 4. The blockage ratio was 1.18%, falling well below the maximum allowable 3 % (Calautit and Hughes, 2014). These placements facilitate proper airflow, prevent backflow, and ensure vortex generation. Ansys meshing tool was used to create the mesh, generating unstructured polyhedral cells—a common practice to enhance the representation of complex geometries, as depicted in Figure 4. The overall mesh comprised 5,065,560 elements with 25,060,512 nodes. Face sizing was applied to faces with a defined element size of 0.3 m, with a transition ratio of 0.272. The computational domain exhibited size gradations from 0.3 m near walls to an increase up to 5 m near boundaries, with

DOI: 10.6092/issn.2281-4485/20043

cell growth rates starting at 1.1 near the model and gradually reaching a rate of 1.2 near the domain's boundaries. Mesh inflation ensured smooth flow, especially near building surfaces, see Figure 4. In a numerical solution, the accuracy should remain unaffected by the number of cells in the discretized domain. To validate numerical results, a grid independence test was conducted for the 0° case of February. The pressure coefficient profile was plotted across a horizontal line in the middle of Face A, indicated by a centreline in Figure 4. Initially, the computational mesh for our domain consisted of approximately 2 million elements. Starting with 2 million elements, three denser grids were tested under identical conditions. As grid density increased, see Figure 5, Cp stabilized at 3 million elements, confirming reliable results with varying mesh sizes. A finer mesh with 5,065,560 elements was chosen for accuracy and efficiency.

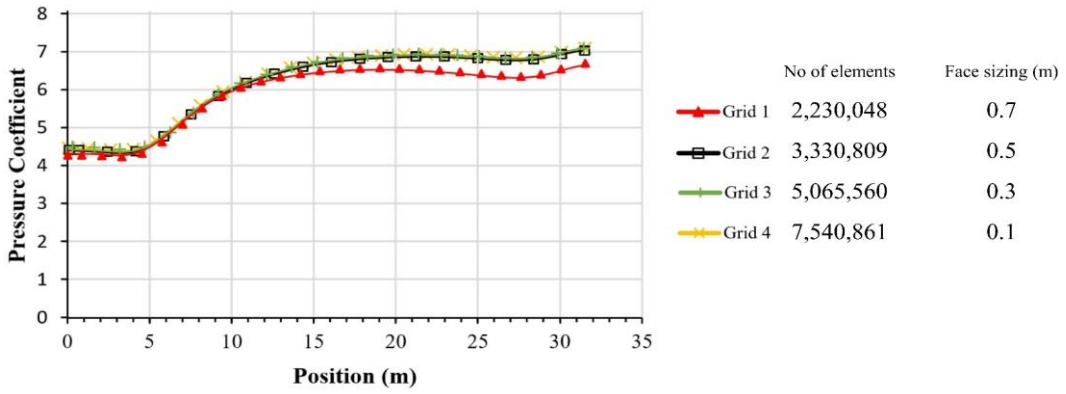

Figure 5
Mesh independence test for all grids

Validation of the CFD Model

The analysis of airflow patterns inside the courtyard building with CFD requires thorough validation to ensure the credibility of the chosen turbulence model, which significantly affects the results. Conducting an empirical or experimental study specific to our research would be valuable but is challenged by limited resources and access to necessary measurement instruments. Therefore, we have addressed this gap by using existing literature and available data, a common approach in prior investigations (Rabeharivelo et al., 2022 , Karimimoshaver et al., 2023).

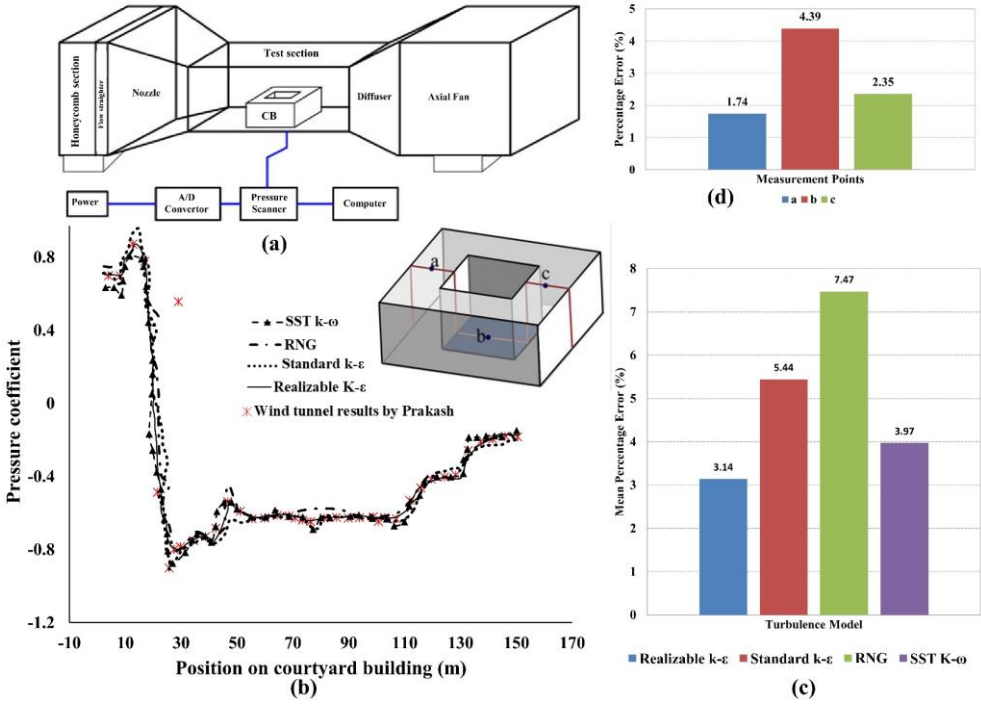

Figure 6
(a) Wind tunnel test by Prakash (2023),
(b) Validation of the Cp profiles around the building between the experimental data and CFD simulation,
(c) Mean average error percentage for CFD turbulence models,
(d) Percentage error for calculated velocity at points a, b, and c.

DOI: 10.6092/issn.2281-4485/20043

To validate our selected turbulence model, we first applied it to a well-documented wind tunnel test flow problem by Prakash (2023) (Prakash, 2023). In this test, a courtyard building with dimensions 50 m × 50 m and a height of 25 m, with a courtyard space of 16.75 m × 16.75 m × 25 m, was analysed using k-ε and SST turbulence models for the same flow phenomenon. The validation procedure focused on assessing the *Cp*, along a red line around the building, see Figure 6, to correlate with experimental results, and measuring velocity at building locations a, b, and c. A comparison with experimental data showed that while the SST model is commonly used and yields superior result (Ai and Mak, 2014 , van Hooff et al., 2017 , Blocken, 2018), the realizable k-ε model results demonstrated a high level of agreement with Prakash's findings, with an average percentage error of 3.14%. For locations a, b, and c, the maximum deviation for velocity using the realizable k-ε model was 4.39% from wind tunnel measurements. The slight error between the two results can be attributed to limitations in the turbulence model and uncertainties in experimental data, confirming that the accuracy of the employed CFD method for subsequent simulations is reliable for predicting airflow behavior in different models.

Results and Discussion

As discussed in the first section, we examine how building orientation affects airspeed and flow patterns within the courtyard and internal spaces. This involves increasing ventilation rates while minimizing turbulence, primarily by boosting air velocity in the courtyard. Air velocity and flow patterns at the 1.7m level were plotted for four building orientations. The airflow speed and distribution inside the courtyard are color-coded using a CFD color map, deemed effective for deriving simulation results. Additionally, significant pressure differences on the building facades also improve ventilation rates within the spaces. To quantify this, average pressure differences were calculated on the classroom facades.

Qualitative analysis

Velocity contours in the model, prepared along plan A-A within the scope of the study, are analysed to identify areas with minimal velocities, indicating locations where the velocity gradually decreases to around 0 m/s. Additionally, vectors representing fluid particle paths, with vector size denoting velocity magnitude, provide a visual representation of the air distribution within the courtyard space. Flow patterns of each month for different wind incidence angles along plan A-A and section B-B are illustrated below. Months with duplicated wind directions are excluded from the qualitative analysis study (highlighted in Table 1) as they exhibit the same airflow patterns, but they will be included in the quantitative results due to variations in wind speed values. The simulation results for January in Figure 7 reveal substantial variations in calculated velocity vectors within the courtyard space across the four scenarios. In the first scenario, where the building orientation is at 0°, airflow patterns exhibit a favourable distribution, with nearly symmetrical flowlines until the generation of vortices. A small stagnant air region appears at the left corner due to air colliding with the windward Face A. This leads to the formation of a small vortex inside the courtyard space in front of the wall, while the central region experiencing minimal impact. With the increase in angle of rotation from 0° to 45°, a significant change in wind patterns inside the courtyard becomes apparent. It is noticeable that the size of the air vortex increases, diminishing airflow velocity within the courtyard, as depicted in the contour plot. The vector plots in section B-B reveal that in front of the windward Face A in the 0° case, a small stagnation point is observed at the bottom of the building. Better airflow performance is observed at the air inlets, with a high amount of air impacts along the courtyard wall near the windward side, deflecting toward the building's roof. It predominantly encounters positive pressure with minor negative pressure near its edges caused by flow separation. The opposite Face B (leeward side) experiences negative pressure attributable to wake effects. As we change from 0° to 15° and then 30°, there is an increase in stagnant flow area size, culminating in the generation of a vortex at 45° which deflects towards the bottom space of the courtyard and captures more regions than before. This stagnant zone is also visible in cases 15° and 30° but with a relatively smaller size, contributing to lower velocity. Hence, for January, the 0° scenario could be a good orientation according to wind flow pattern results. In February, the results closely resemble those of January due to minor variations in wind direction impact, see Figure 8. Consequently, the results for this month tend to favor the first scenario due to its superior performance regarding airflow patterns (same results for December). This

DOI: 10.6092/issn.2281-4485/20043

preference is based on its optimal distribution of wind velocities inside the courtyard and its lower incidence of vortices within both the courtyard and the main windward facades. Upon examining the results for March, with a significant change in the wind direction impact on the building compared to previous months, the distinction among the four scenarios becomes more pronounced. This is particularly noticeable in the velocity vector plans within the courtyard. The stagnant points for airflow cover a larger area in the scenarios with 0°, 30°, and 45°, unlike the 15° scenario, which exhibits a more

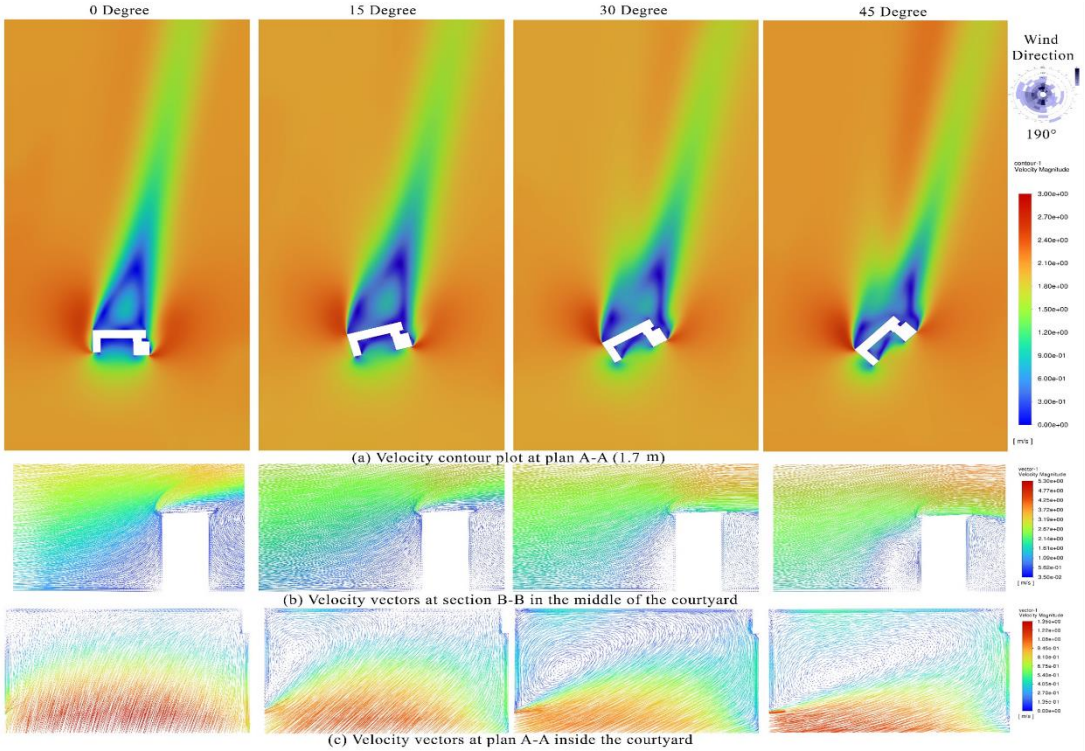

Figure 7
Simulation results of January (Wind Direction : 190°)

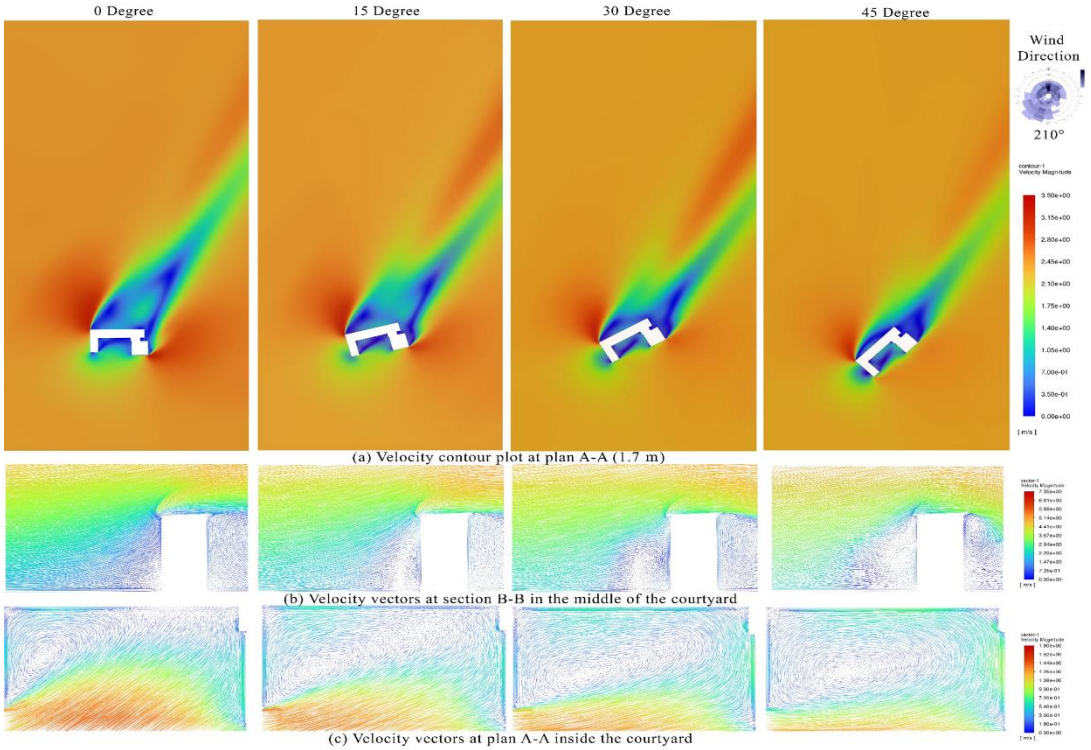

Figure 8
Simulation results of February (Wind Direction : 210°)

DOI: 10.6092/issn.2281-4485/20043

favorable airflow distribution with higher speeds within the courtyard, as depicted in the velocity contour plot in Figure 9. Regarding section B-B, a relative similarity is observed among the four cases, with a slightly smaller vortex size in the 45° scenario compared to the other cases. Additionally, larger

favorable airflow distribution with higher speeds within the courtyard, as depicted in the velocity contour plot in Figure 9. Regarding section B-B, a relative similarity is observed among the four cases, with a slightly smaller vortex size in the 45° scenario compared to the other cases. Additionally, larger

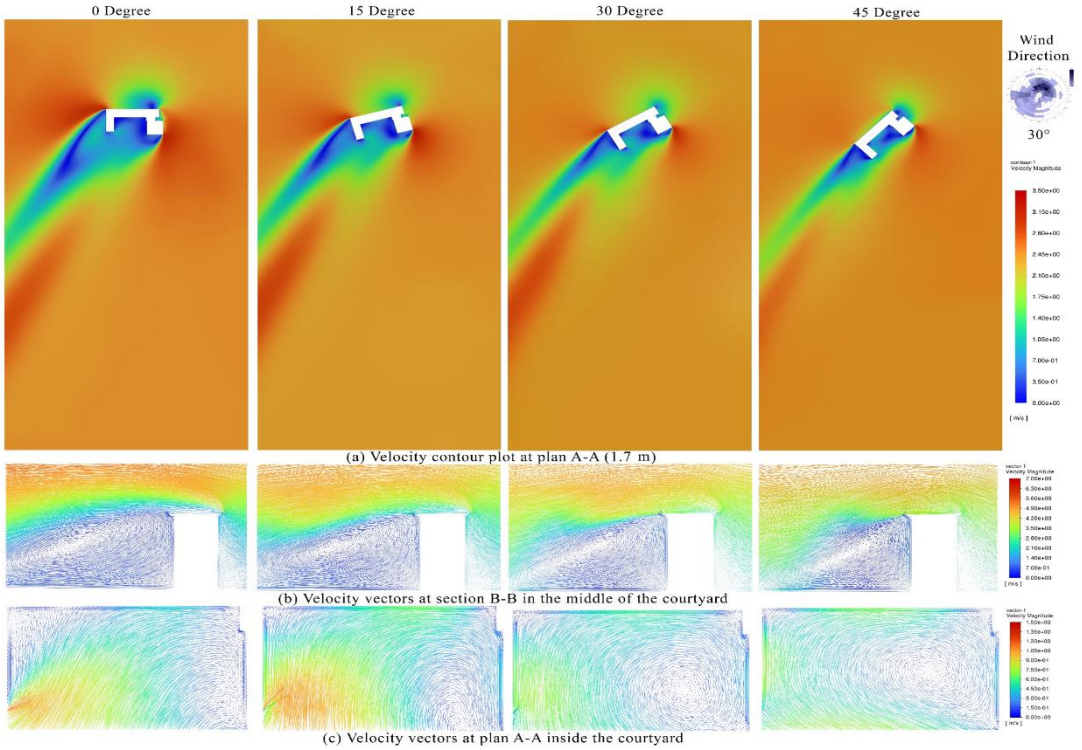

Figure 9
Simulation results of March (Wind Direction : 30°)

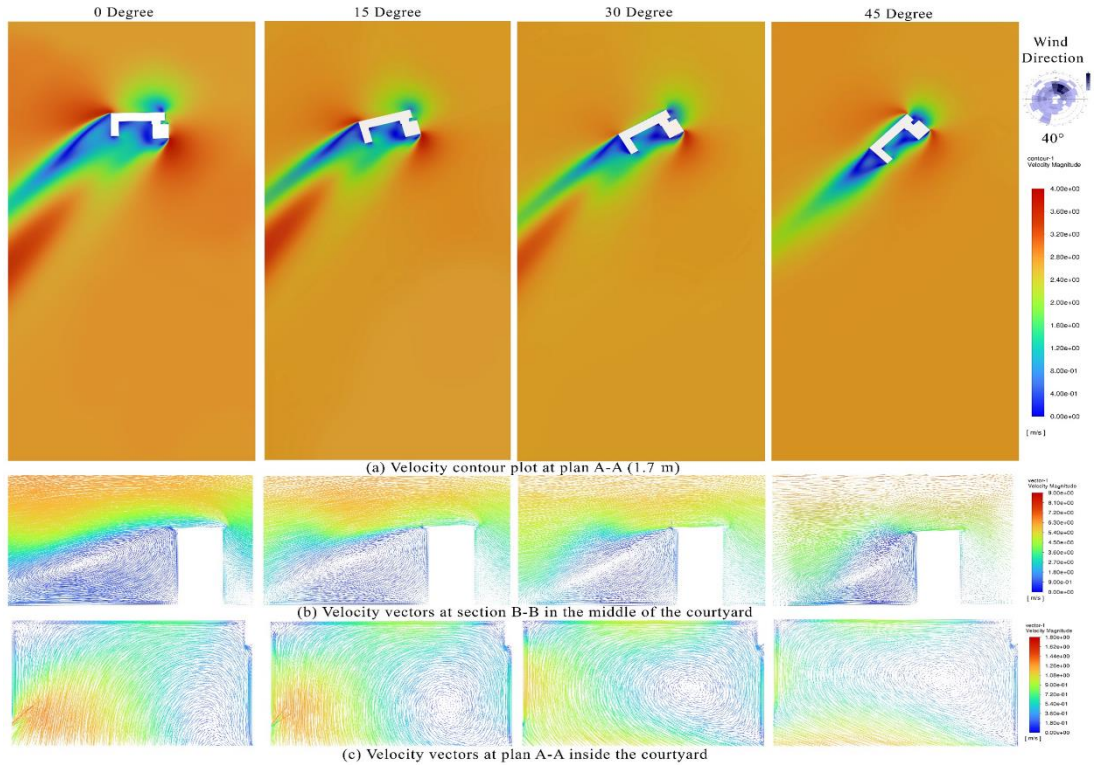

Figure 10
Simulation results of April (Wind Direction : 40°)

DOI: 10.6092/issn.2281-4485/20043

stagnant air zones are present on the leeward side of the building. Therefore, in these scenarios, the optimal airflow speed and distribution within the courtyard appears to be at 15° (same results for May). Reviewing the results for April in Figure 10, it is clear that the 45° scenario conspicuously stands out as the least favorable case, both in terms of air velocities and their distribution within the courtyard space. In contrast, the 0° and 15° scenarios distinctly exhibit superior performance (same results for October).

In June, we observed similar results across all four scenarios for both plan A-A and section B-B, in

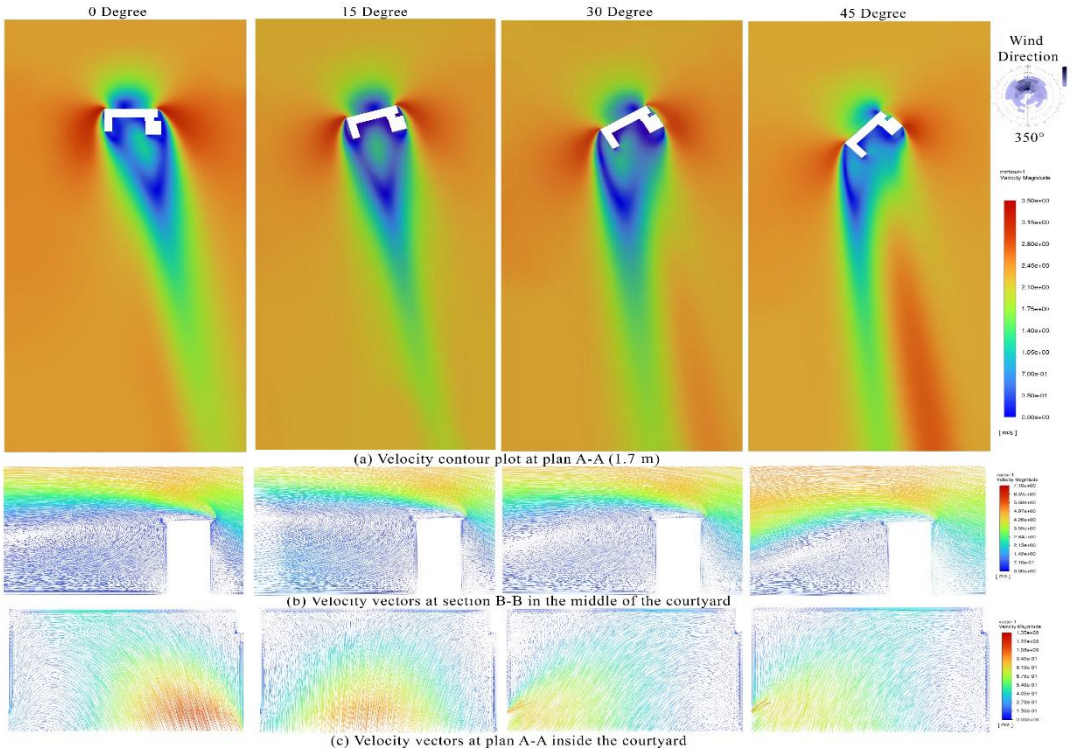

Figure 11
Simulation results of June (Wind Direction : 350°)

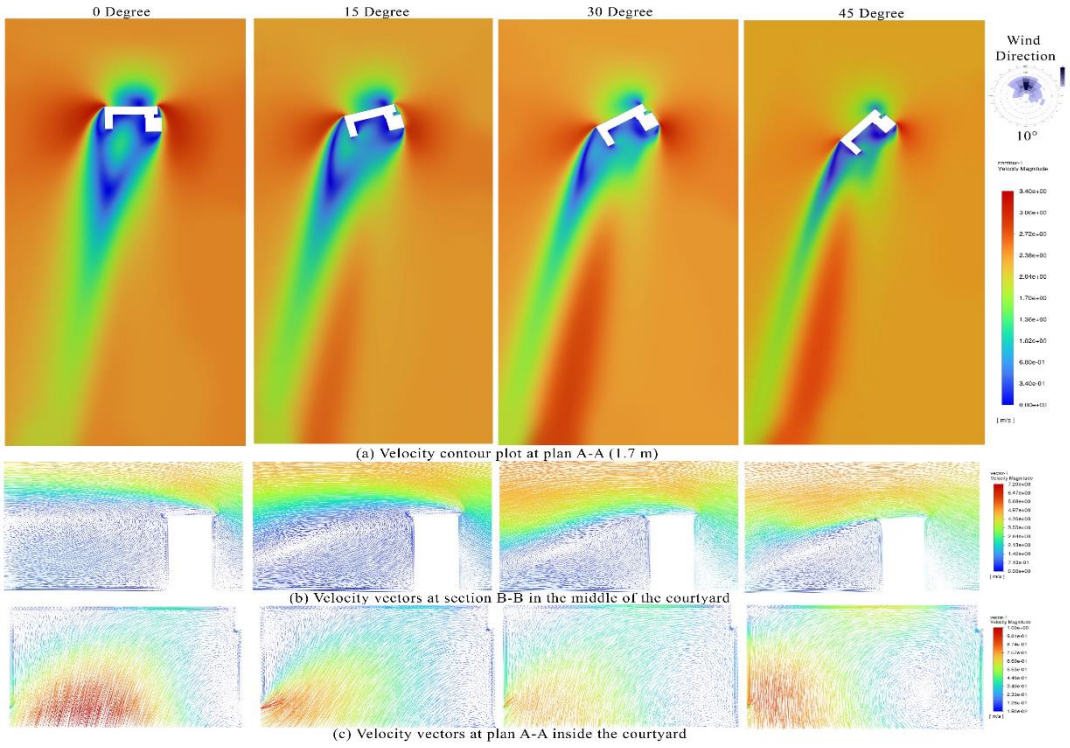

Figure 12
Simulation results of September (Wind Direction: 10°)

DOI: 10.6092/issn.2281-4485/20043

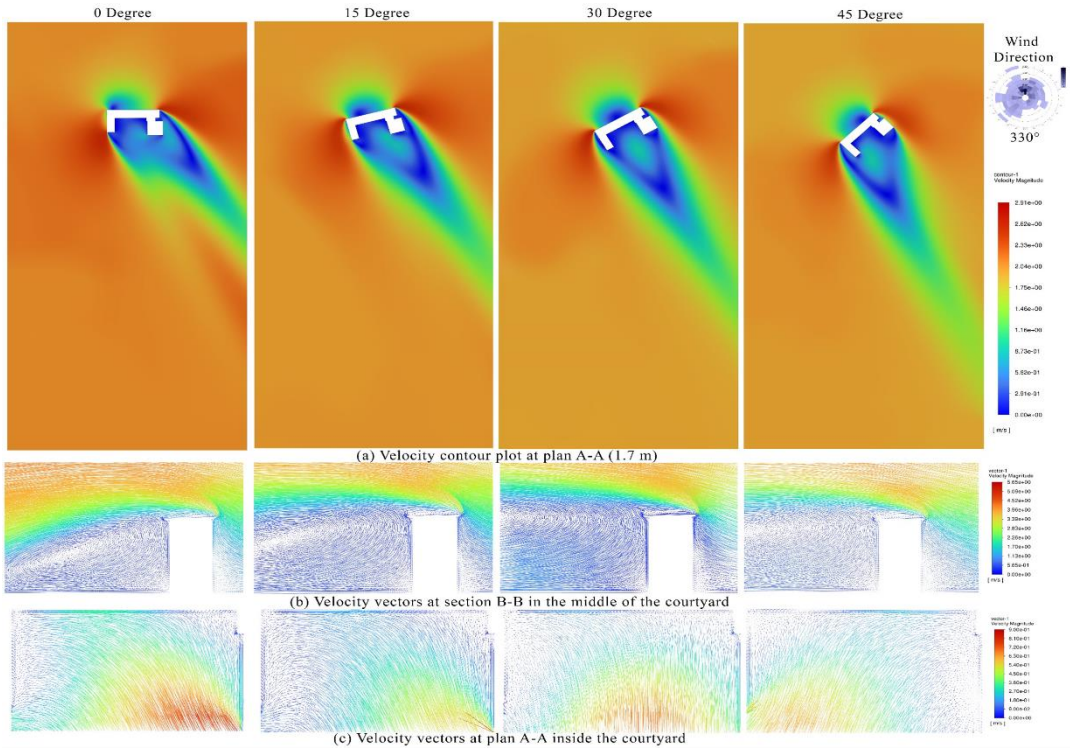

Figure 13
Simulation results of November (Wind Direction: 330°)

terms of the distribution and velocities of air at different wind flow angles. It's important to note that there were slightly higher velocity regions in the 0° and 15° cases, as depicted on the contour plot in Figure 11 (similar results are observed for July and August). Examining the results for September in Figure 12, we also observe that the 0° and 15° scenarios show superior performance in the patterns and distribution of air velocities within the courtyard. In all the cases, there are similarities in the area of recirculation behind the leeward wall, the separation of flow at the upper edge of the wind-facing wall, and the shear layer. The performance begins to decline with the 30° scenario and reaches its lowest point in the 45° scenario concerning airflow distribution. As we reach the month of November, the 0° and 15° scenarios demonstrate the superior distribution of airflow patterns and velocities within the courtyard. Remarkably, the 0° scenario performs slightly better than the 15° scenario in terms of velocity, see Figure 13.. As can be seen, the orientation becomes more significant in this context. According to CFD results,, the courtyard with zero orientation demonstrates the best wind flow pattern, allowing high-velocity wind to enter and circulate properly inside. However, even increasing the rotation up to 15° also yields good results compared to 30° and 45°, which significantly decrease airflow performance

Quantitative analysis

Two parameters were compared among the different cases: average air velocity of the courtyard and static pressure differences of Faces A and B of the building. Figure 14 presents the average air velocities magnitude inside the courtyard for the 1.7m plan of each scenario. In most cases, higher average velocity values are observed for both 0° and 15° scenarios, exhibiting a more consistent velocity magnitude than the 30° and 45° scenarios where a drop in velocity magnitude is demonstrated due to the formation of recirculation zones within the courtyard area. The highest air velocity in the model reaches 0.87 m/s in February. According to ASHRAE standards, the calculated average wind speed was extremely low, ranging between 0.36 and 0.87 m/s for the best scenario (0°). Additionally, as stated by the Beaufort scale, these conditions would be felt by standing users as a gentle breeze. In the latter, as shown in Figure 14, average pressure differences between windward and leeward sides of the classrooms in the building model were calculated to predict airflow and ventilation rates inside following the Bernoulli's principle of fluid dynamics. The results showed that in most months, the highest-pressure differences were found in the 0° scenario followed by the second scenario, whereas the pressure differences were lowest at 45°.

DOI: 10.6092/issn.2281-4485/20043

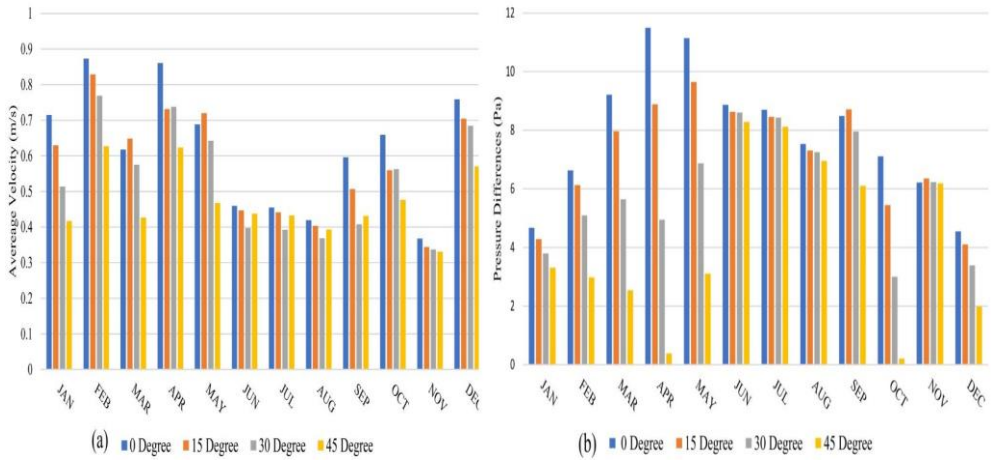

Figure 14
(a)Average air velocities inside the courtyard at 1.7 m level for different cases (b)Average pressure differences between two main facades of the classrooms for different cases

Conclusions

In conclusion, this research endeavors to address the challenges posed by the prevalent standardization of educational building models in Egypt, which often neglect the diverse climatic conditions across regions. Focusing on the crucial aspect of ventilation performance in buildings, we employed a CFD simulations to investigate the impact of different courtyard orientations on airflow patterns and ventilation efficiency within a representative educational building model located in the hot-arid climate of Cairo and Delta region. Our numerical study, encompassing four building orientation scenarios (0° , 15° , 30° , and 45°) in the northwest direction, offers valuable insights into the potential enhancements in natural ventilation for courtyard buildings in hot-arid climates. Through the meticulous application of the Reynolds-averaged Navier-Stokes (RANS) equations and choosing an appropriate turbulence model, we navigated the complexities of CFD simulations, opting for computational efficiency while maintaining the reliability of results. The results of our analysis indicated that the 0° and 15° orientations in the northwest direction significantly enhance airflow within the courtyard, fostering improved ventilation rates within the internal spaces. Furthermore, the calculated pressure differences on the building facades highlight the significance of wind-induced ventilation, emphasizing the potential for improved airflow rates in the 0° scenario. Meanwhile, 30° and 45° represent unfavorable airflow directions due to insufficient wind amplification. The recommendations outlined in this paper can be applied to any building utilizing natural ventilation for thermal comfort, given they share analogous architectural configurations as well as comparable weather conditions.

Nomenclature

◦	degree
ω	specific dissipation rate
i, j	mean velocity component in the xi-directions
μt	turbulence viscosity
ε	turbulence dissipation rate
μ	dynamic viscosity
p	pressure (Pa)
ϱ	air density (kg/m3)
VABL*	atmospheric boundary layer friction velocity
t	time (s)
z0	aerodynamic ground roughness length
Z	positional coordinate along with the building's height
k	von Kármán constant
Vref	the reference wind speed
Href	the reference height
I(z)	turbulent intensity
a	surface roughness coefficient
Cp	pressure coefficient
Subscripts and abbreviation	
BWh	Hot-Arid desert
BSh	Semi-Arid Hot
HBRC	Housing and Building National Research Centre
EREC	Egyptian Residential Energy Code
BS	Dry Semiarid (Steppe)
CFD	Computational Fluid Dynamics
GAEB	General Authority for Educational Buildings
RANS	Reynolds-averaged Navier-Stokes
EPW	EnergyPlus Weather File Format
RLZ	Realizable k-epsilon model
LES	Large Eddy Simulation
SKT	Standard k-epsilon model
RNG	Renormalized group k-epsilon
PBNS	Pressure-Based Navier-Stokes
SST	Shear Stress Transport
Pa	Pascal
ABL	Atmospheric Boundary Layer

DOI: 10.6092/issn.2281-4485/20043

Conflict of interest

The authors have no competing interests to declare that are relevant to the content of this article.

References

ABDELHADY M.I.M. (2021) Numerical simulation for the geometrical courtyard parameters affecting the indoor natural ventilation, case study in Sur, Oman. Journal of Xi'an University of Architecture Technology, 13(3):1-15. https://doi.org/10.37896/JXAT13.3/30500

ABDIN T., MAHMOUD A.H.A. (2017) A checklist for the assessment of energy performance of public schools in Cairo, Egypt. Paper presented at the International Conference for Sustainable Design of the Built Environment-SDBE London.

AFANDI G.E. (2014) Evaluation of NCEP climate forecast system reanalysis (CFSR) against surface observations over Egypt. American Journal of Science and Technology, 1(4), 157-167. https://www.aascit.org/journal/archive2?journalId=902&paperId=724

AI Z.., MAK C.M. (2014) Modeling of coupled urban wind flow and indoor air flow on a high-density near-wall mesh: Sensitivity analyses and case study for single-sided ventilation. Environmental modelling software, 60, 57-68. https://doi.org/10.1016/j.envsoft.2014.06.010

ALMAJIDI B.H., HAMEED T.M. (2020) The role of the Internal courtyard in organizing the function and shaping architecture. Association of Arab Universities Journal of Engineering Sciences, 27(2):135-146. https://doi.org/10.33261/jaaru.2020.27.2.012

ASHRAE - American Society of Heating R. & Air-Conditioning, E. (2017). ASHRAE Standard 55 thermal environmental conditions for human occupancy.

BIENVENIDO-HUERTAS D., DE LA HOZ-TORRES M.L., AGUILAR A.J., TEJEDOR B., SÁNCHEZ-GARCÍA D. (2023) Holistic overview of natural ventilation and mixed mode in built environment of warm climate zones and hot seasons. Building and environment, 245: 110942. https://doi.org/10.1016/j.buildenv.2023.110942

BLOCKEN B. (2018) LES over RANS in building simulation for outdoor and indoor applications: A foregone conclusion? Paper presented at the Building Simulation.

CALAUTIT J.K., HUGHES B.R. (2014) Wind tunnel and CFD study of the natural ventilation performance of a commercial multi-directional wind tower. Building and environment, 80:71-83. https://doi.org/10.1016/j.buildenv.2014.05.022

CAPMAS (2023) Statistics of the number of students in schools, Egypt. CAPMAS, Central Agency for Public Mobilization & Statistic, Statistics of the number of students in schools, Egypt, 2023. Cairo: Central Agency for Public Mobilization & Statistic: Egyptian government

ELNABAWI M.H., HAMZA N., DUDEK S. (2017) Shading Historical Commercial Streets in Hot Arid Areas: Questioning the Common Wisdom. Paper presented at the Proceedings of the 33rd PLEA International Conference: Design to Thrive, PLEA, Edinburgh, UK.

GAEB (2023) General Authority of Educational Buildings, prototypes after the earthquake, Architectural design department, Researches and studies administration, Egypt. In. Egypt.

GB50009 (2012) Ministry of Housing Urban-Rural Construction of the People's Republic of China, Load code for the design of building structures, Haidian District, Beijing, China. In. Urban-Rural Construction of the People's Republic of China, Haidian District, Beijing, China.

GIVONI B. (1998) Climate considerations in building and urban design: John Wiley & Sons. 0471291773: 0471291773

HAMED R. (2023) The role of built environment in fostering the safety of children with autism in public primary schools. (Master of Science In Interior Design Master), University of Oklahoma, Graduate College. Retrieved from https://hdl.handle.net/11244/337535

IBRAHIM M. W., ALBUKHARI I.N., TOULAH A.S. O., IBRAHIM S.W. (2021) The Inner Courtyard and Its Role in Activating the Sustainable Dimension of Residential Buildings in Hot Regions. Journal of Al-Azhar University Engineering Sector, 16(58):101-126. https://doi.org/10.21608/auej.2021.141780

KARIMIMOSHAVER M., SADATHOSSEINI M., ARAM F., AHMADI J., MOSAVI A. (2023) The effect of geometry and location of balconies on single-sided natural ventilation in high-rise buildings. Energy Reports, 10: 2174-2193. https://doi.org/10.1016/j.egyr.2023.09.030

MAHMOUD A.H.A. (2011). An analysis of bioclimatic zones and implications for design of outdoor built environments in Egypt. Building and environment, 46(3): 605-620. doi:Ayman Hassaan A. Mahmoud

MINISTRY OF HOUSING (2005) Energy efficiency non residential building code, ECP-306, Utilities and Urban Communities, Housing and Building National Research Center, HBRC, Egypt

DOI: 10.6092/issn.2281-4485/20043

MOHAMED M. (2010) Traditional ways of dealing with climate in Egypt. In The Seventh International Conference of Sustainable Architecture and Urban Development (SAUD 2010): The Center for the Study of Architecture in Arab Region (CSAAR Press).

MOHAMED M.A., EL-AMIN M F. (2022) Inward and Outward Opening Properties of One-Sided Windcat-chers: Experimental and Analytical Evaluation. Sustaina-bility, 14(7):4048. https://doi.org/10.3390/su1407 4048

OBEIDAT L.M., ALREBEI O.F., NOUH MA'BDEH, S., AL-RADAIDEH T., AMHAMED A.I. (2023) Parametric Enhancement of a Window-Windcatcher for Enhanced Thermal Comfort and Natural Ventilation. Atmosphere, 14(5):844. :https://doi.org/10.3390/atmos 14050844

PERÉN J., VAN HOOFF T., LEITE B.C.C., BLOCKEN B. (2015) Impact of eaves on cross-ventilation of a generic isolated leeward sawtooth roof building: Windward eaves, leeward eaves and eaves inclination. Building and environment, 92:578-590. https://doi.org/10.1016/j.buildenv.2015.05.011

PRAKASH D. (2023) Ventilation performance analysis on low-rise courtyard building for various courtyard sha-pe factors and roof topology. International Journal of Ventilation, 22(1): 56-76. https://doi.org/10.1080/ 14733315.2022.2036477

RABEHARIVELO R., KAVRAZ M., AYGÜN C. (2022) Thermal comfort in classrooms considering a traditional wind tower in Trabzon through simulation. Paper presented at the Building Simulation.

RIVAS E., SANTIAGO J.L., MARTÍN F., MARTILLI, A. (2022) Impact of natural ventilation on exposure to SARS-CoV 2 in indoor/semi-indoor terraces using CO_2 concentrations as a proxy. Journal of Building Engineering, 46:103725. https://doi.org/10.1016/j.jobe.2021.10 3725

SALEEM A.A., ABEL-RAHMAN A.K., ALI A.H.H. OOKAWARA S. (2016) An analysis of thermal comfort and energy consumption within public primary schools in Egypt. IAFOR J. Sustain. Energy Environ, 3. https://doi.org/10.22492/ijsee.3.1.03

SERRA N. (2023) Revisiting RANS turbulence model-ling used in built-environment CFD simulations. Building and Environment, 237: 110333. https://doi.org/10.1016/ j.buildenv.2023.110333

SOFLAEI F., SHOKOUHIAN M., TABADKANI A., MOSLEHI H., BERARDI U. (2020) A simulation-based model for courtyard housing design based on adaptive thermal comfort. Journal of Building Engineering, 31: 101335. https://doi.org/10.1016/j.jobe.2020.101335

STASI R., RUGGIERO F., BERARDI U. (2024) Influence of cross-ventilation cooling potential on thermal comfort in high-rise buildings in a hot and humid climate. Building and environment, 248:111096. https://doi.org/ 10.1016/j.buildenv.2023.111096

TALEB H.M., ABUMOEILAK L. (2021) An assessment of different courtyard configurations in urban communities in the United Arab Emirates (UAE). Smart Sustainable Built Environment, 10(1): 67-89. https://doi. org/10.1108/SASBE-08-2019-0116

TALEB H.M., WRIEKAT T., HASHAYKEH H. (2020) Optimising natural ventilation using courtyard strategies: CFD simulation of a G+ 1 office building in Madinah. International Journal of Sustainable Energy, 39(7):659-684. https://doi.org/10.1080/14786451.2020.1748027

TANG C., LIANG T., NONG G. (2023) Impacts of convection on the thermal performance of radiant heating system with novel dry radiant module. Building and environment, 238: 110370. https://doi.org/10.1016/j.buil denv.2023.110370

TOMINAGA Y., MOCHIDA A., YOSHIE R., KATAOKA H., NOZU T., YOSHIKAWA M., SHIRASAWA T. (2008) AIJ guidelines for practical applications of CFD to pedestrian wind environment around buildings. Journal of Wind Engineering Industrial Aerodynamics, 96(10-11):1749-1761. https://doi.org/10. 1016/j.jweia.2008.02.058

VAN HOOFF T., BLOCKEN B., TOMINAGA Y. (2017) On the accuracy of CFD simulations of cross-ventilation flows for a generic isolated building: Comparison of RANS, LES and experiments. Building and environment, 114:148-165. https://doi.org/10.1016/ j.buildenv.2016.12.019

WAZERI U. (2002) Practices on environmental archi-tecture-the sunny design for the interior court-Studies on Cairo and Toshki. Cairo, Madboli.

YAWEN Z., WEI Y., YONGHAN L., XIAOLI H., SHAOBO Z., QIAOYUN H., SHUANGPING D. (2023) Evaluation of building arrangement on natural ventilation potential in ideal building arrays. Journal of Asian Architecture and Building Engineering, 22(6):1-23. https://doi.org/10.1080/13467581.2023.2191680

ZHANG X., WEERASURIYA A.U., TSE K.T. (2020) CFD simulation of natural ventilation of a generic building in various incident wind directions: Comparison of turbulence modelling, evaluation methods, and ventilation mechanisms. Energy Buildings, 229, 110516. https://doi.org/10.1016/j.enbuild.2020.110516